AIP | Applied Physics Letters

Surface wave resonances supported on a square array of square metallic pillars

S. J. Berry, T. Campbell, A. P. Hibbins, and J. R. Sambles

Citation: Appl. Phys. Lett. **100**, 101107 (2012); doi: 10.1063/1.3691949

View online: http://dx.doi.org/10.1063/1.3691949

View Table of Contents: http://apl.aip.org/resource/1/APPLAB/v100/i10

Published by the American Institute of Physics.

APPLIED PHYSICS LETTERS **100**, 101107 (2012)

Surface wave resonances supported on a square array of square metallic pillars

S. J. Berry,[1,a)] T. Campbell,[2] A. P. Hibbins,[1] and J. R. Sambles[1]
[1]*Electromagnetic Materials Group, School of Physics, University of Exeter, Exeter EX4 4QL, United Kingdom*
[2]*BAE Systems, Warton Aerodrome, 392A, Warton, Preston PR4 1AX, United Kingdom*

(Received 3 November 2011; accepted 11 February 2012; published online 6 March 2012)

A family of transverse-magnetic surface waves is shown to be supported at microwave frequencies by a square array of subwavelength square cross-section metal pillars on a conducting ground plane. These surface waves are experimentally characterised with a collimated microwave beam apparatus that utilises a pair of two-dimensional parabolic mirrors positioned on the sample surface. The dispersion of the modes, each associated with a quantisation of the electromagnetic field in the depth of the slits, is fully characterised and compared with the predictions of finite element modelling. © *2012 American Institute of Physics*. [http://dx.doi.org/10.1063/1.3691949]

Planar metal surfaces are well known to support electromagnetic surface waves at frequencies from the radio to the ultra-violet.[1–3] Any penetration of the electromagnetic fields into the metal (i.e., skin depth) induces a boundary condition at its surface that localises these surface waves to the interface between the dielectric and the metal, with electromagnetic fields that decay exponentially into each material. At visible frequencies, the surface wave, normally referred to as a surface plasmon polariton (SPP),[4] is tightly confined within distances of the order of the wavelength in the dielectric and much less than the wavelength in the metal. By contrast at microwave frequencies, where metals can often assumed to be perfectly conducting, the surface wave supported by a planar metal-dielectric interface is unconfined in the dielectric. However, it has been shown[5–8] that subwavelength structuring of the metal surface produces field confinement at microwave frequencies, which means that the structured surface now behaves much more like a planar metallic one at optical frequencies with tight confinement of the electromagnetic fields. This is the concept of "spoof" or "designer" surface plasmons. The essence is that for frequencies below the cutoff frequency, υ_{cutoff}, the decay length into the subwavelength holes is much greater than the skin depth of the unstructured metal thereby allowing the textured metal surface to become rather like the "poorer" conductor it is at optical frequencies.[6] This leads to much tighter confinement of this surface wave in an analogy to the SPP supported at visible wavelengths. Of course, above υ_{cutoff}, there is a family of transverse-electric eigenmodes which are quantised in the z-direction due to the onset of propagating solutions within the holes. A family of surface waves may then be supported with asymptotic frequencies being defined by this quantisation.

In contrast to the hole array discussed above, a square array of subwavelength square cross-section metal pillars on a conducting ground plane supports transverse electromagnetic (TEM) waveguide modes within the slits and thus has no lower cut-off frequency. However, the TEM waveguide modes supported within the slits are also quantised in the z-direction, which again leads to a family of bound surface waves with asymptotic frequencies equal to the resonant frequencies of the modes in the slits. These waveguide modes are analogous to the waveguide modes supported between a pair of parallel metal plates. Therefore, the structure will give a response which is similar to that of the higher order waveguide modes supported above the cut-off frequency of the aforementioned hole array,[9–12] where the lowest energy quantisation will occur when a quarter wavelength resonance is supported in the slit cavity.

The experimental sample is cut from a single block of aluminium 460 × 460 mm^2, with square bottomed slits cut to a depth of 30 mm with all of the resulting square metallic pillars remaining connected to the conducting ground plane. Each square pillar has side lengths of $w_P = 3$ mm with the slit width between pillars being $w_S = 1$ mm (Figure 1). The pitch (λ_g) of the structure is 4 mm in both the x and y directions giving the onset of diffraction in the air above the sample as $\upsilon = 37.5$ GHz, for grazing incident radiation azimuthal angles of $\phi = 0°$ or $90°$. We consider only non-radiating surface modes in this study and therefore, it is straightforward to increase the onset of diffraction (to further increase the range of the non-diffracting domain) by changing the azimuthal angle to $\phi = 45°$. At this angle, the onset of diffraction occurs at $\upsilon = 53$ GHz. To decrease the resonant frequencies of the modes within the slits, the slits are filled with paraffin wax ($\epsilon_r \approx 2.3$), thereby increasing the

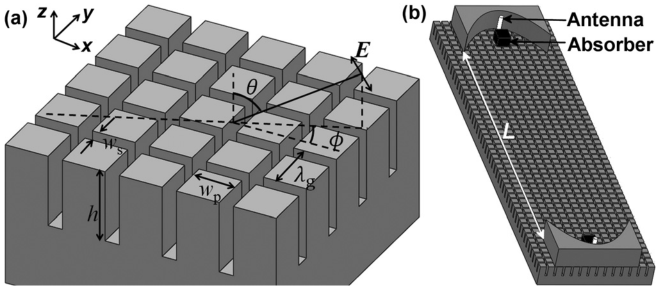

FIG. 1. Schematic diagrams of the (a) bi-grating structure and (b) the experimental setup. White cylinders indicate the position of the antenna and the black boxes indicate the positions of the absorbers.

[a)] Author to whom correspondence should be addressed. Electronic mail: sjb221@ex.ac.uk.

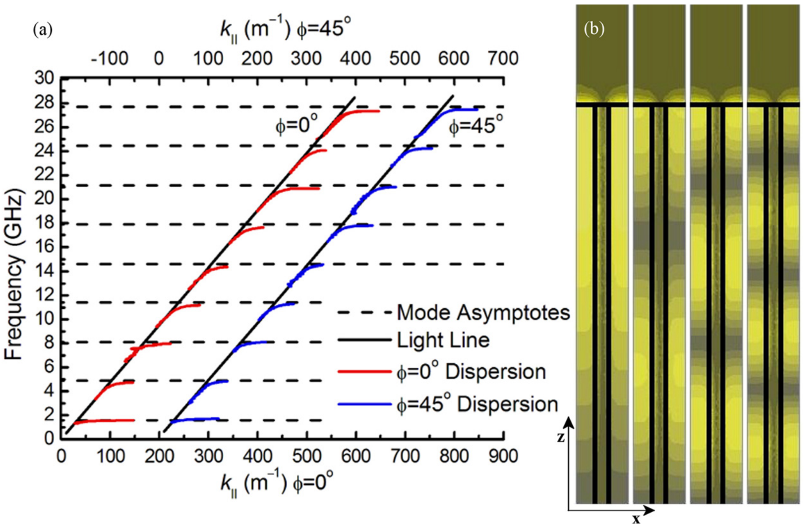

FIG. 2. (Color online) (a) Plot showing the experimental dispersion of the first nine modes of the structure together at $\phi = 0°$ and $\phi = 45°$ (displaced by $+200\boldsymbol{k}_{||}$) with the predictions of the resonant frequencies from numerical modelling (horizontal dashed lines). (b) Plots of the time averaged electric field intensity for the first four modes at the resonant frequency of the mode, where light indicates high field and dark indicates low field.

number of modes available for study in the non-diffracting regime.

The surface waves are excited and detected using stripped coaxial antennas, in the frequency range well below the fundamental resonance of the antenna, to provide near-field coupling to the surface mode. They are designed to minimise free space radiating energy at the frequencies of interest which limits direct transmission, through the dielectric, between the antennas. Each antenna is placed at the focal point of a two dimensional parabolic mirror which thereby collimates the surface wave and directs it across the surface. A second identical parabolic mirror is used to then collect and refocus the collimated surface wave onto the receive antenna. The distance between the two parabolic mirrors on the surface is defined as L and is approximately 30 cm. In front of (along the direct line of sight between) both the receive- and detect-antennas is placed a small amount of microwave absorber to prevent any direct path signal across the surface of the sample.

The phase of the transmitted signal is recorded using a vector network analyser for two different distances between the source and the receive antennas, L_1 and L_2. By using two distances and obtaining the differences in phase shifts for the two situations, the phase shifts brought about at the coupling-in and coupling-out structures are eliminated. Thereby the wavevector $k_{||}$, required for the derivation of the surface mode's dispersion, is obtained simply from the phase change $(\phi_2 - \phi_1)$ over the distance $(L_2 - L_1)$ as given below

$$k_{||} = \frac{2\pi}{L_2 - L_1}\left(\frac{\phi_2 - \phi_1}{2\pi} + m\right),$$

Here, m is an unknown integer since the system measures the phase only to modulo 2π. This unknown integer m is however readily obtained by changing it in unit steps and examining how it impacts the resulting dispersion curve which, away from any resonance, has to lie close to the light line.

The modes of the system are related to quantisation of the electromagnetic field within the depth of the slits. Boundary conditions for such resonances are an approximate $\boldsymbol{E}$-field maximum at the surface and an $\boldsymbol{E}$-field minimum at the ground plane. Therefore, these resonances occur whenever the external wavelength approaches $\lambda = \frac{(2N-1)h\sqrt{\epsilon_r}}{4}$, where N is an integer. This sets up a resonant standing wave in the cavity and no power propagates across the sample since all of the power is localised within the cavity resonance. Thus, a family of surface waves is supported with asymptotic frequencies equal to those of the cavity resonances which because of the square symmetry are largely unaffected by the azimuthal angle of the sample. Modelled fields of the first four modes supported by the system are shown in Figure 2, calculated using a finite element method (FEM) modelling package.[13]

The group velocity of each mode decreases as the resonant condition is approached tending to zero at the asymptote. This decrease in group velocity together with the limited range of in-plane momentum ($k_{||}$) of the incident field (from diffraction at the excitation dipole) eventually leads to a complete loss in received power as the mode approaches the asymptote preventing the quantification of the dispersion very close to the resonant frequency. The dispersion of the modes measured at both $\phi = 0°$ and $\phi = 45°$ is highly similar, showing the azimuthal independence. Further both agree extremely well with both the shape of the dispersion and the

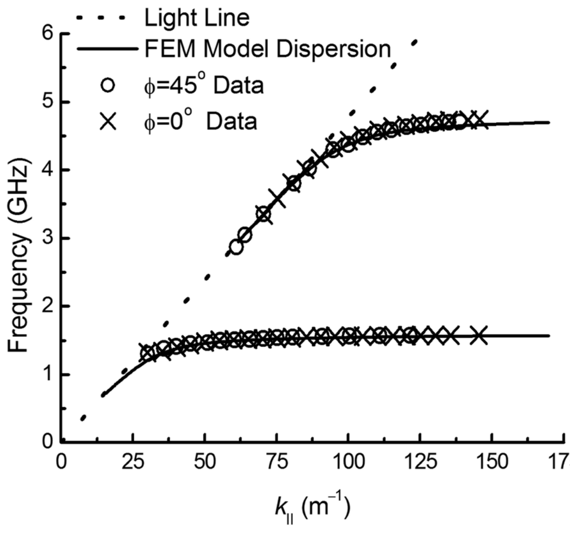

FIG. 3. Plot of the dispersion for the first two modes of the structure at both azimuth angles $\phi = 0°$ (crosses) and $\phi = 45°$ (circles) along with the FEM modelled dispersion (black lines).

asymptotes obtained from FEM modelling as illustrated in Figures 2 and 3. In addition, the electromagnetic fields shown in Figure 2 illustrate clearly the quantisation as well as the obvious surface wave character of the modes. Figure 3 shows in detail the measured and predicted dispersions of the first and second modes demonstrating fully that these are surface wave like in character with wavevectors extending well beyond the light line. This also shows fully the agreement between the shape and position of the FEM dispersion curve and the experimental data. The lowest order mode is only quantified down to about 1.3 GHz as the wavelength of the microwaves (23 cm) is now becoming comparable to the overall size of the system.

In conclusion, the dispersion of surface waves on a square array of square cross-section metal pillars has been measured by exploiting a two dimensional parabolic mirror technique for creation and detection of collimated surface waves. The results show that a family of surface waves may be supported by pillar or crossed slit structures rather than just holes even though there is no lowest cut-off frequency. A family of TM modes has been shown to exist with dispersion which asymptotes to frequencies defined by the pillar heights (slit depth) and the refractive index of the material filling the slits. The concept of "designer" surface plasmons at microwave frequencies has thereby been extended experimentally to a further class of structured metamaterial surfaces.

The authors acknowledge the support of BAE Systems and EPSRC.

[1] H. M. Barlow and A. L. Cullen, Proc. IEE, **10**, 329 (1953).
[2] R. Colin, *Field Theory of Guided Waves*, 2nd ed. (Wiley, New York, 1990), Chap. 7
[3] W. L. Barnes, A. Dereux, and T. W. Ebbesen, Nature **424**, 824 (2003).
[4] R. H. Ritchie, Phys. Rev. **106**, 874 (1957).
[5] J. B. Pendry, L. Matrin-Morenzo, and F. J. Garcia-Vidal, Science **305**, 847 (2004).
[6] A. P. Hibbins, B. R. Evans, and J. R. Sambles, Science **308**, 670 (2005).
[7] F. J. García-Vidal, L. Martín-Moreno, and J. B. Pendry, J. Opt. A, Pure Appl. Opt. **7**, S97 (2005).
[8] E. Hendry, A. P. Hibbins, and J. R. Sambles, Phys. Rev. B **78**, 235426 (2008).
[9] T. Jiang, L. Shen, X. Zhang, and L. Ran, Prog. Electromagn. Res. **8**, 91 (2009).
[10] M. Qiu, Opt. Express **13**, 7583 (2005).
[11] Z. Ruan and M. Qiu, Appl. Phys. Lett. **90**, 201906 (2007).
[12] H. J. Rance, I. R. Hooper, A. P. Hibbins, and J. R. Sambles, Appl. Phys. Lett. **99**, 187107 (2011).
[13] ANSOFT HFSS$^{\mathrm{TM}}$, Ansoft Corporation, Pittsburgh, PA.